Local field potential

Alain Destexhe and Claude Bedard (2013), Scholarpedia, 8(8):10713. doi:10.4249/scholarpedia.10713 revision #135811 [link to/cite this article]

- **Alain Destexhe**, CNRS, France
- **Claude Bedard**, CNRS, Gif-sur-Yvette, France

The **local field potential** (LFP) refers to the electric potential in the extracellular space around neurons. The LFP is a widely available signal in many recording configurations, ranging from single-electrode recordings to multi-electrode arrays. In this article, we review the main properties of the LFP as well as different types of LFP models.

Contents

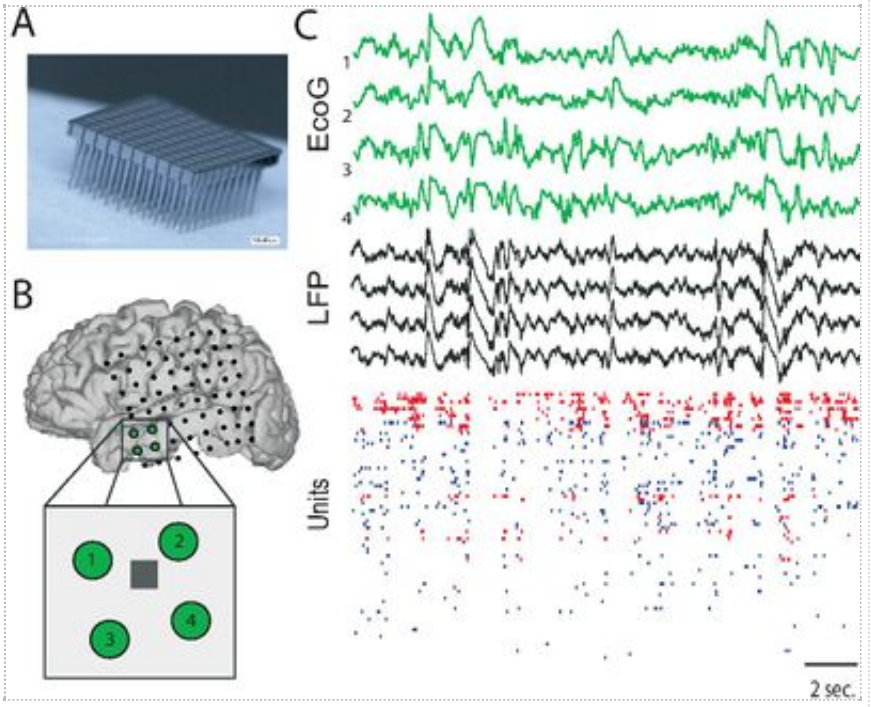

Figure 1: Local field potentials recorded in humans using an array of extracellular electrodes. A. Array of 100 silicon electrodes (Utah array, BlackRock systems), with 400 μm inter-electrode distance, and which can be inserted into cerebral cortex. B. Plan of implementation of surface electrodes (black dots). Inset: magnified view of the medial temporal lobe, with four surface electrodes (green) and the Utah array (gray square). C. Typical recordings obtained with surface electrodes (EcoG, green), local field potentials (LFP) and identified neurons (Units; red=inhibitory, blue=excitatory). The 4 nearby surface EcoG are shown (green), while 4 randomly chosen LFPs were shown among all the electrodes available. This example was recorded during slow-wave sleep, and one can see slow delta waves in the surface EcoG as well as in the LFPs, and also modulate the firing of units (modified from Peyrache et al., 2012).

8 Internal links

Introduction

The Local Field Potential (LFP) is the electric potential recorded in the extracellular space in brain tissue, typically using micro-electrodes (metal, silicon or glass micropipettes). LFPs differ from the electroencephalogram (EEG), which is recorded at the surface of the scalp, and with macro-electrodes. It also differs from the electro-corticogram (EcoG), which are recorded from the surface of the brain using large subdural electrodes, while LFPs are recorded in depth, from within the cortical tissue (or other deep brain structures).

Besides their invasive aspect, LFPs also sample relatively localized populations of neurons, as these signals can be very different for electrodes separated by 1 mm (Destexhe et al., 1999) or by a few hundred microns (Katzner et al., 2009). In contrast, the EEG samples much larger populations of neurons (Niedermeyer and Lopes da Silva, 1998). The difference is due to the fact that the EEG signals must propagate through various media, such as cerebrospinal fluid, dura matter, cranium, muscle and skin, and are therefore much more subject to filtering and diffusion phenomena across these media. However, even if recorded close to the neuronal sources, LFP signals are also filtered, because the recording electrode is separated from the sources by portions of cortical tissue. Besides these differences, EEG and LFP signals display the same type of oscillations during wake and sleep states (Steriade, 2003).

Early studies demonstrated that action potentials have a limited participation to the genesis of the EEG or LFPs. The initial theory about the genesis of the EEG and LFP oscillations, the "circus movement theory", postulated that the frequency of oscillations was due to travelling pulses along loops of connected neurons (Rothberger, 1931; Bishop, 1936). Bremer (1938, 1949) was an opponent to this theory and he was the first to propose that the EEG is not generated by action potentials but rather by oscillations of the membrane potential of neurons. Eccles (1951) proposed that LFP and EEG activities are generated by summated postsynaptic potentials arising from the synchronized excitation of neurons. Intracellular recordings from cortical neurons later demonstrated a close correspondence between EEG/LFP activity and synaptic potentials (Klee et al., 1965; Creutzfeldt et al., 1966a, 1966b). The current view is that EEG and LFPs are generated by synchronized synaptic currents arising on cortical neurons, possibly through the formation of dipoles (Niedermeyer and Lopes da Silva, 1998; Nunez and Srinivasan, 2005).

One of the possible explanation for the fact that action potentials have a limited participation to EEG and LFP activities is that the cortical tissue exerts strong frequency-filtering properties. High frequencies (greater than ≈ 100 Hz), such as that produced by action potentials, are subject to steep attenuation, while low-frequency events, such as synaptic potentials, attenuate less with distance. Consequently, the extracellular image of action potentials is visible only for electrodes immediately adjacent to the recorded cell, while synaptic events may propagate over large distances in extracellular space and be recordable as far as on the surface of the scalp, where they participate to the genesis of the EEG. This frequency-dependent behavior is a property routinely seen in extracellular recordings of neuronal units: the amplitude of extracellularly-recorded spikes is very sensitive to the position of the electrode, presumably because action potentials are visible only for the cell(s) immediately adjacent to the electrode. By contrast, slow events presumably originate from synaptic events in a large number of neighboring neurons, and thus are more stable to small changes of electrode position. This property is fundamental to allow one to resolve single units from extracellular recordings.

In this article, we review the main spatial and temporal (or spectral) properties of LFPs, as well as different ways to model them.

Local field potentials in human and animal recordings

In this section, we review the main properties of LFPs in different experimental preparations.

Spatial and temporal properties of LFPs

Figure 1A shows an example of one of the most popular extracellular multi-electrode array systems, called the "Utah array", developed at the University of Utah and by BlackRock Microsystems. This 100-electrode array was implemented in human medial temporal cortex together with surface electrodes (Fig. 1B). The surface electrodes record the electrocorticogram (EcoG in Fig. 1), which record the electric potential at the surface of the cortex (green signals in Fig. 1C). By contrast, the LFP provides a recording of the electric potential from within the brain tissue, and samples a more local population of neurons (black signals in Fig. 1C). One can clearly see slow delta waves that are visible both in the surface EcoG and in depth LFP recordings (this example was recorded during slow-wave sleep). A number of discriminated units are also shown, and were recorded using the same set of electrodes.

Figure 2 shows LFPs recorded by 8 sets of bipolar tungsten electrodes from cat parietal cortex during wake and sleep states. The LFP displays the same essential features as classically seen from the EEG: during wakefulness, the LFP was dominated by low-amplitude fast-frequency "desynchronized" activity (Fig. 2A), while during slow-wave sleep, the LFP displayed high-amplitude slow waves (Fig. 2B). During Rapid-Eye Movement (REM) sleep (Fig. 2C), the LFP reverts back to desynchronized activity with nearly identical characteristics as during wakefulness. Note that, contrary to the EEG, the LFP signals are not contaminated by muscular (EMG) activity, and therefore constitute ideal signals for detailed analyses, even at high frequencies. For instance, it was shown that the high similarity between Wake and REM states extends to about everything that can be measured electrophysiologically, such as the spectral content, the correlation dynamics and the unit activity (Destexhe et al., 1999). On the other hand, slow-wave activity is clearly different, as shown for example by their different pattern of coherence as a function of distance compared to the fast activity of wake and REM states. This difference can be quantified by calculating spatial correlations, and in particular their decay with distance. As expected from the LFP signals, the correlations remained high for larger distances only during slow-wave sleep (Fig. 2, middle panels). In contrast, the temporal correlations displayed similar profiles between different brain states (Fig. 2, right panels).

Relation between LFP and neuronal activity

The relationship between LFP and the firing of neurons depends on the brain state, as illustrated in Fig. 3. During wakefulness, the low-amplitude fast-frequency LFP was associated with sustained and very irregular firing activity in the units (Fig. 3A,B, Wake). There was no apparent relation between units and LFP by visual inspection, although a statistical analysis revealed that the depth-negative deflections were on average related to an increase of firing activity in the units (Fig. 3C, Wake; see details in Destexhe et al., 1999). During slow-wave sleep, the ensemble activity was surprisingly similar to wakefulness, although more bursty (Fig. 3A, SWS). However, at closer scrutiny (Fig. 3B), it appears that synchronous "silences" in all the units occur systematically and simultaneously with the depth-positive part of the slow-wave (Fig. 3B, SWS; blue shaded area). This type of synchronized silence is often

referred as "Down-state", and was also visible in the human recordings (see Fig. 1C). This modulation of firing by the slow wave is also visible when computing the statistical relation between units and slow-waves (Fig. 3C, SWS). The tight relation between slow waves and Up and Down states in single neurons was firmly demonstrated using intracellular recordings in natural slow-wave sleep in cats (Steriade et al., 2001; reviewed in Steriade, 2003). The human and cat recordings display essentially the same features of the relation between LFPs and neuronal units.

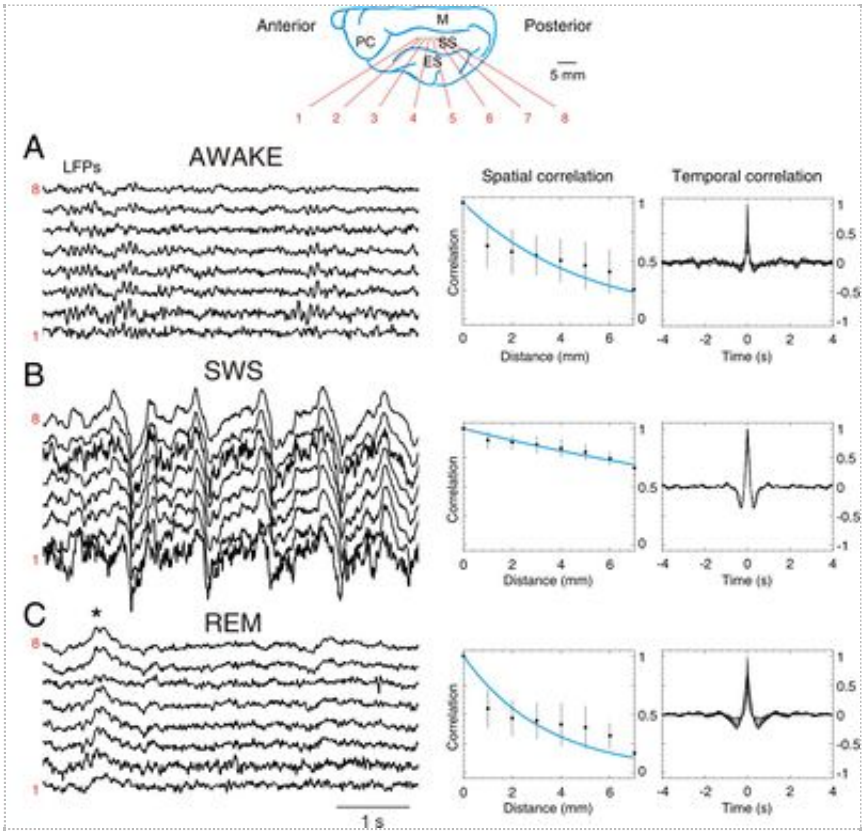

Figure 2: Local field potentials in cats during wake and sleep states. Eight bipolar tungsten electrodes (inter-electrode distance of 1 mm) were inserted into the depth (1 mm) of areas 5-7 of cat parietal cortex (suprasylvian gyrus, area 5-7; see top scheme for arrangement of electrodes). Local field potentials (LFPs) are shown (left panels) together with a representation of the correlations as a function of distance (Spatial correlations; middle panels) and time (Temporal correlations; right panels). A. When the animal was awake, LFPs were characterized by low-amplitude fast activities in the beta/gamma frequency range (15-75 Hz). Correlations decayed steeply with distance and time. B. During slow-wave sleep, the LFPs were dominated by large-amplitude slow-wave complexes recurring at a low frequency (<1 Hz; up to 4 Hz). Correlations stayed high for large distances. C. During episodes of REM sleep, LFPs and correlations had similar characteristics as during wake periods (* indicates a PGO wave). Modified from Destexhe et al., 1999.

Power spectra and frequency scaling of LFPs

One of the characteristics of EEG and LFP signals is that their power-spectrum exhibits $1/f$ frequency scaling at low frequencies, as shown by a number of studies (Bhattacharya, 2001; Bedard et al., 2006a; Novikov et al., 1997; Pritchard, 1992; Dehghani et al., 2010a). Figure 4 illustrates such scaling in the human EEG and in the LFP recorded with tungsten electrodes in cat parietal cortex, both when the subject was awake and attentive. In these conditions, the low-frequency end of the PSD scales as $1/f$ (red lines). A more detailed study showed that the EEG scaling exponent varies from 1 to 2 according to the brain region considered (Dehghani et al., 2010a).

The origin of such $1/f$ "noise" is at present unclear. $1/f$ spectra can result from self-organized critical phenomena (Jensen, 1998), suggesting that neuronal activity may be working according to such states (Beggs and Plenz, 2003), but this subject is controverted (Bedard et al., 2006a; Dehghani et al., 2012). The morphology of the neuron may also be responsible for filtering in the $1/f$ to $1/f^2$ range (Pettersen and Einevoll, 2008), but this scaling applies to high frequencies and cannnot explain the $1/f$ scaling at low frequencies. Finally, the $1/f$ scaling may be due to filtering properties of the currents through extracellular media (Bedard et al., 2006a). This conclusion was reached by noting that the global activity reconstructed from multisite unit recordings scales identically as the LFP if a "$1/f$

filter" is assumed, and without the need to assume self-organized critical states in neural activity (Fig. 5). However, the latter study made the point that $1/f$ filter may be necessary to explain the experimental results, but no mechanism was provided to explain such a $1/f$ filter. We will see below that ionic diffusion may explain these observations.

Modeling LFPs

The LFP is generated by electric currents and charges in brain cells, including neurons and glial cells. In particular, all ionic currents in neurons can potentially contribute to the LFP. The main contribution to LFPs is believed to be the synaptic currents in neurons, although intrinsic voltage-dependent currents and spikes can also contribute. Today's prevalent model is that EEG and LFPs are generated by synchronized synaptic currents arising on cortical pyramidal neurons, possibly through the formation of dipoles (Niedermeyer and Lopes da Silva, 1998; Nunez and Srinivasan, 2005). The LFP also interacts with the extracellular medium, trough several mechanisms, such as capacitive effects, polarization, or ionic diffusion. These types of interaction confer specific frequency dependence of the extracellular electric potential, and thus are important for correctly interpreting the LFP. In this section, we review different models of LFPs, from simple to more complex models.

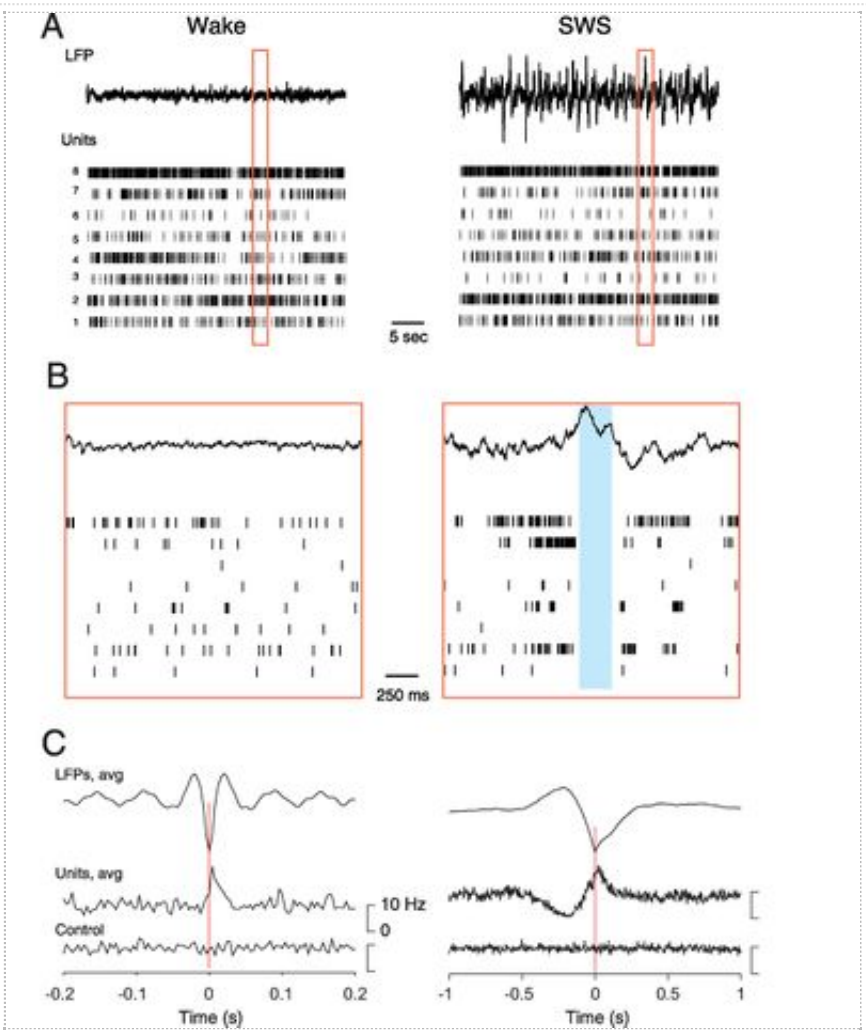

Figure 3: Relation between LFP and unit activity in different brain states. A. *Left:* During wakefulness, the low-amplitude fast-frequency LFP activity is associated with highly irregular firing activity of the 8 multi-units recorded simultaneously (same experimental setup as in Fig. 2). *Right:* During slow-wave sleep (SWS), the activity is similar as wakefulness, except that synchronized "silences" of firing activity occur in all cells simultaneously, and in relation to the slow waves. B. Same activity as in A at 20 times higher temporal resolution. The blue shaded area indicates the synchronized silence ("Down state") simultaneous in all cells, and occurring in parallel with slow waves. C. Wave-triggered averages of spiking activity. During wakefulness, the LFP negative

The simplest model of LFP

The simplest model for LFP generation assumes that the LFP is generated by transmembrane currents and that neurons are embedded in a perfectly resistive medium (also called Ohmic medium, such as salted water, with no capacitive or other component). This is equivalent to assume that the electric conductivity σ and permittivity ϵ of the extracellular medium

are constant everywhere and do not depend on frequency. In this case, one first considers the electric potential generated by a punctual current source. Combining Ohm's law with the charge conservation law, and considering a spherical symmetry, we obtain:

$$V(r) = \frac{1}{4\pi\sigma}\frac{I_0}{|r - r_0|},$$

where $V(r)$ is the extracellular potential at a position r in extracellular space, I_0 is the current source, and $|r - r_0|$ is the absolute distance between r and the position of the current source r_0.

According to this model, it is easy to verify from the Equation above that $V(r)$ is solution of Laplace equation:

$$\nabla^2 V = 0.$$

Because the principle of linear superposition applies, the potential resulting from a set of current sources is given by:

$$V(r) = \frac{1}{4\pi\sigma}\sum_j \frac{I_j}{|r - r_j|}.$$

peaks were correlated with an increased firing activity in the units. During SWS, the negative peak of the slow wave was correlated with a strong decrease of firing in the units (Down state), followed by a rebound a sustained activity (Up state). Modified from Destexhe et al., 1999.

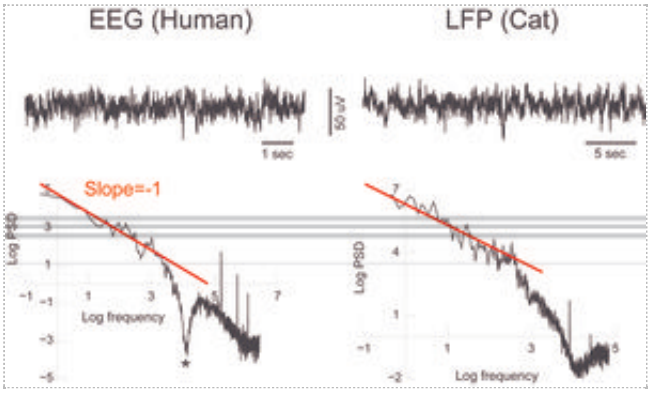

Figure 4: $1/f$ scaling of EEG and LFP signals. The top traces show examples of human EEG recordings (left, vertex EEG) and LFP recording from cat parietal cortex (right) during awake and attentive states. The corresponding power spectra (lower panels) display approximate $1/f$ scaling at low frequencies. The straight lines (red) indicate a slope of -1 in this log-log representation. The signals were not filtered, except for a notch filter at 60 Hz (*) for the EEG, and the data acquisition filters at high frequencies (not visible at this scale).

This equation will be referred to as the "standard model".
This expression can be used to calculate the LFP resulting from complex morphologies, or from networks of neurons. This model is widely used to model extracellular potentials, since early models (Rall and Shepherd, 1968) to today's models of extracellular activity (Protopapas et al., 1998; Destexhe, 1998; Nunez and Srinivasan, 2005; Gold et al., 2006; Pettersen and Einevoll, 2008).

This model is also called the "point current source model". A variant of this model, called the "line-source approximation" (Holt and Koch, 1999), in which the membrane current source of a cylindric compartment is evenly distributed along a line corresponding to the axis of the cylinder, and which constitutes a more accurate approximation for compartmental models.

Example of LFPs generated by a simple model

To illustrate the standard LFP model, we consider a model of the genesis of absence seizures in the thalamocortical system (Destexhe, 1998). This type of generalized epileptic seizure generates typical EEG patterns consisting of "Spikes" and "Waves", oscillating at a frequency around 3 Hz. Spike-and-wave patterns are seen in many other types of epileptic seizures as well (Niedermeyer and Lopes da Silva, 1998). To model such seizures, it is necessary to take into account the complex intrinsic firing properties of cortical and thalamic neurons, as well as the different types of receptors present in the system. In particular, this model showed that an increase of cortical excitability can give rise

to absence seizures with spike-and-wave patterns (Destexhe, 1998; see details in the Spike-and-Wave Oscillations Scholarpedia article). In this model, the spike-and-wave patterns were generated using the standard model (see above), using a linear arrangement of pyramidal (PY) neurons (20 μm intercellular distance), where I_j was the transmembrane current of each pyramidal neuron, excluding the currents responsible for action potentials (see details in Destexhe, 1998). The simulation showed that spike-and-wave patterns can be reproduced by this simple model, where synchronized postsynaptic potentials (EPSP/IPSP sequences) generate the negative "spike", while slow positive currents (also synchronized) generate the slow positive "wave" (Fig. 6). This illustrates that the standard model of LFPs can generate the spike-and-wave patterns typically seen during seizures.

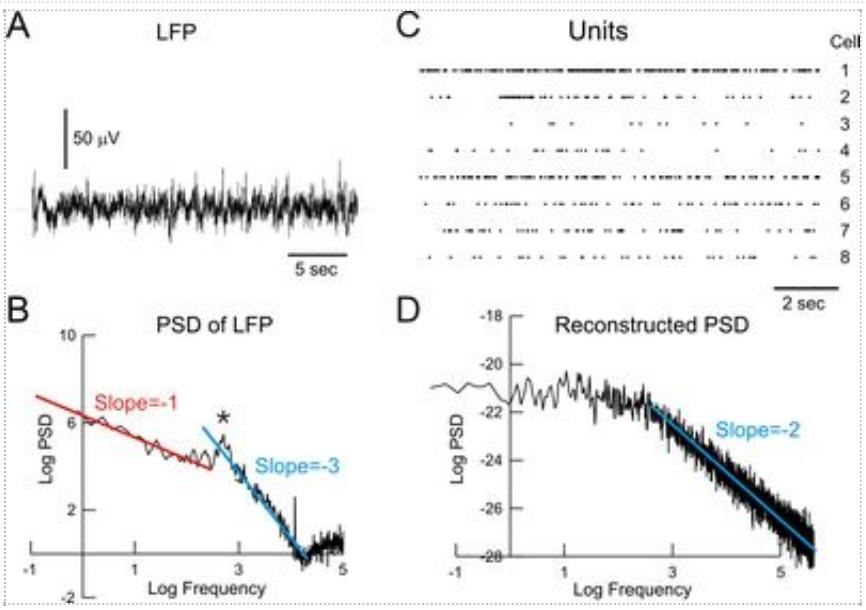

Figure 5: Failure to reconstruct LFP power spectra from unit activity. A. LFP recording in awake cat parietal cortex (same recording as in Fig. 4, left). B. Power spectral density (PSD) of the LFP, showing two scaling regions, $1/f$ at low frequencies (red line, slope=-1), and $1/f^3$ at high frequencies (blue line; slope=-3). C. Unit activity from the same experiment, recorded with a system of 8 tungsten electrodes. D. Attempt to reconstruct the LFP signal from the unit activity. The low frequency end of the PSD was constant (zero slope), while the high-frequency end scaled as $1/f^2$ (blue line, slope=-2). An exponent of -1 is missing to reproduce the LFP scaling (modified from Bedard et al., 2006a).

Frequency filtering properties of LFPs

As mentioned in the introduction, the fact that action potentials have little participation to the LFP may be explained by frequency-filtering properties of the extracellular medium. If the medium acts as a low-pass filter, it may attenuate more severely the high frequencies (greater than $\approx$ 100 Hz), such as that produced by action potentials, while the attenuation will be less severe for lower frequencies such as synaptic events. As a consequence, an extracellular electrode at a given position will "see" only the action potentials for cells immediately adjacent to the electrode. On the other hand, the low-frequencies of the LFP will be a compound signal of slower events (such as synaptic events) from a very large population of cells.

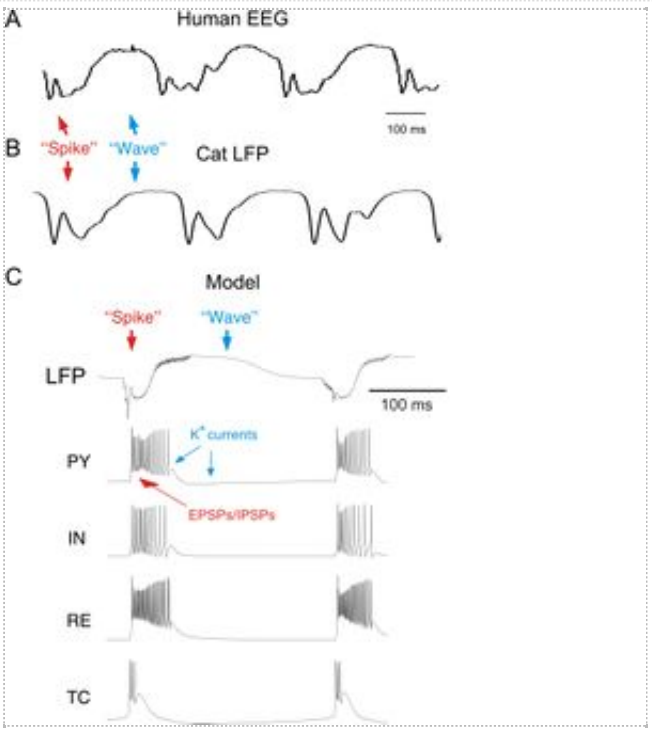

Figure 6: Modeling spike-and-wave LFPs from a thalamocortical network model of absence seizures.

It is important to realize that the fact that spikes are only visible for cells laying within a few microns from the electrode is the property that allows one to resolve single units. If there were no such frequency-dependent behavior, extracellular recordings would always be dominated by a signal where thousands of units contribute, and it would be impossible to distinguish a given unit in such multi-unit activity. Thus, frequency filtering is a great opportunity for the experimentalist.

A. Spike and wave oscillations in human EEG during an absence epileptic seizure. B. Spike and wave oscillations in the LFP recorded using a tungsten electrode in the parietal cortex of an epileptic cat. C. Computational model of spike and wave oscillations. The model consists of a network of single-compartment Hodgkin-Huxley type model neurons, where synaptic interactions were modeled by conductance-based kinetic models of glutamate (AMPA, NMDA) and γ-amino-butyric acid ($GABA_A$ and $GABA_B$) synaptic receptors. Reducing the fast ($GABA_A$ -mediated) inhibition in cortex resulted in the emergence of hyper-synchronized oscillations at a frequency of around 3 Hz. The LFP was calculated from monopolar sources (pyramidal neurons only) using all ionic currents except the fast I_{Na} /I_K currents involved in spike generation. The model LFP generated the typical spike-and-wave patterns seen experimentally during seizures. When all cells fired in synchrony, the LFP generated a negative "spike", while the neuronal silences were associated with a slow positive "wave". The "spike" was generated by the synchronized EPSP/IPSP sequences, while the "wave" was generated by slow K^+ currents in pyramidal neurons (arrows). PY = cortical pyramidal neurons, IN = cortical interneurons, RE = thalamic reticular neurons, TC = thalamic relay cells. Modified from Destexhe, 1998; see details in the Spike-and-Wave Oscillations Scholarpedia article.

How to model frequency-filtering properties?

Several possible origins for the frequency-filtering properties of LFPs have been proposed. As mentioned above, it was proposed that the morphology of the neuron is responsible for some type of filtering (Pettersen and Einevoll, 2008; Linden et al., 2010). In this case, the return current, which participates to generating the LFP, is filtered by the membrane and therefore gives rise to filtered LFPs. However, it was also shown (Bedard et al., 2010) that this type of filtering is only present for isolated inputs, and disappears for *in vivo*--like conditions where the neuron is subject to synaptic bombardment at many synapses simultaneously (see High-conductance State Scholarpedia article). This suggests that, under *in vivo* conditions, the filtering due to morphology can be neglected. Another possible source of filtering is the fact that action potentials could be quadrupoles in dendritic and axonal structures (Milstein and Koch, 2008), and therefore attenuate steeply (quadrupoles attenuate as $1/r^3$ compared to $1/r^2$ with dipoles). This contribution may also participate, although the postulated quadripolar configuration for action potentials still needs to be demonstrated experimentally. Besides, none of these possibilities explain the $1/f$ structure at low frequencies.

A third possible cause for frequency filtering, which was suggested earlier (Bedard et al., 2004), is due to the non-resistive or inhomogeneous properties of extracellular media. We explore this possible cause in more detail below, with several types of extracellular filtering. We will see that some of them can also explain the $1/f$ power spectral structure at low frequencies.

A first type of extracellular frequency filtering is due to electrical non-homogeneity. The extracellular space is not a homogeneous fluid (as assumed in the standard model), but is a compact aggregate of fluids and membranes, as shown by morphological studies (a nice review of the structure of extracellular space, or neuropil, can be found in Peters et al., 1991). In terms of electric properties, because fluids are highly conductive and membranes are excellent insulators, it means that the extracellular space has a highly inhomogeneous electric structure. To correctly model

extracellular space, one must take into account this complex mixture of conductive and non-conductive media, as well as the fact that membranes are capacitors, and therefore the extracellular medium, by its structure, is not a resistor but also contains myriads of capacitors.

How to model such complex and heterogeneous media ? Unfortunately, the equations given above for the standard model cannot be used, because if σ and ϵ depend on space, Laplace equation is not valid anymore. To obtain a consistent formalism, one must restart the model from first principles, the Maxwell equations of electromagnetism. Two approaches are possible, first to design a "microscopic model", in which the microscopic variations of conductivity (and permittivity) are taken into account explicitly, to account for the mixture of fluids and membranes. A second approach is to derive a "macroscopic" (or mean-field) model, in which the extracellular medium is seen as an average of the microscopic properties. Equivalently, one could say that the extracellular medium is viewed with a spatial resolution which is larger than the microscopic variations of conductivity. These two approaches are considered successively below.

Model of LFP in inhomogeneous extracellular space

To design a correct microscopic model, one needs to start from Maxwell equations. This was done previously (Bedard et al., 2004), and the main result is that, in a non-homogeneous medium, the extracellular potential obeys the following equation (written in Fourier frequency space):

$$\nabla \cdot ((\sigma + i\omega\epsilon)\nabla V_{\omega)} = 0.$$

This equation gives the spatial evolution of the ω-frequency component of the extracellular potential, V_ω, as a function of the electric conductivity σ and permittivity ϵ, which both vary in space. This equation is general enough to calculate the propagation of the extracellular potential in extracellular media which can have a complex or inhomogeneous structure.

It is important to note that the equation above reduces to Laplace equation ($\nabla^2 V_\omega = 0$) when the medium is homogeneous with respect to σ and ϵ. Thus, this equation is a generalization of Laplace equation for media where σ and ϵ are non-homogeneous.

This model of non-homogeneous extracellular space was simulated with different spatial profiles of conductivity and permittivity around neurons (Bedard et al., 2004). It was found that according to the spatial profile of σ and ϵ, one can have a high-pass or low-pass filter, but in general when σ is high at short distance of the membrane source, and decays at larger distances from the neuron, then a low-pass filter is observed. For example, if the conductivity decays exponentially with distance from the neuron, a low-pass filter attenuates more strongly the fast frequencies compared to low frequencies. A simulation of the LFP generated in such conditions showed that the extracellular waveform of an action potential changes as the distance to the source is increased (Bedard et al., 2004; see Fig. 7). Thus, this model accounts for basic features of frequency filtering.

Assuming a point current source with a spherical symmetry, one can show that the extracellular potential at a distance R from the source is given by

$$V_\omega = \frac{I_\omega^f}{4\pi\sigma(R)} \int_R^\infty \frac{1}{r'^2} \cdot \frac{\sigma(R) + i\omega\varepsilon(R)}{\sigma(r') + i\omega\varepsilon(r')}\, dr' \ ,$$

where I_ω^f is the free-charge current (in Fourier space). One can see from this equation that the ω-frequency component of the extracellular potential is given by a similar term as in the standard model, $\frac{I_\omega^f}{4\pi\sigma(R)}$, but that this term is modulated by the complex expression in the integral. One can also see from this expression that the result of the integral will be different for different frequencies ω, but only if σ and ϵ are dependent on position. Therefore, the inhomogeneity of σ and ϵ will necessarily create a filtering. Note that if σ and ϵ are constant, the integral equals $1/R$, and one recovers the standard model.

Example of a model of frequency-filtering LFPs

To illustrate the frequency-filtering model explained above, we consider a simulation of the genesis of action potentials and how the corresponding LFP is filtered in extracellular space. We consider a standard Hodgkin-Huxley model of a neuron, together with a model of the extracellular space with spatially-variable conductivity and permittivity. The neuronal membrane is immediately adjacent to a highly conductive extracellular fluid, while at further distances, there is a higher and higher probability of finding low-conductivity obstacles (membranes, vessels). This situation was modelled as a profile where the conductivity is high for short distances (to account for the presence of highly conductive fluid adjacent to the membrane), and decays exponentially with distance. Simulating this model resulted in strong low-pass filtering properties, as illustrated in Fig. 7.

Mean-field model of LFPs

As mentioned above, another approach is to adopt a more macroscopic point of view, and consider a mean-field model of the LFP. A great help for designing mean-field models is that Maxwell equations are invariant under change of scale, if electric parameters σ and ϵ are renormalized appropriately (see details in Jackson, 1999, Bedard and Destexhe, 2011). A mean-field approach is also justified by the fact that the values of σ and ϵ measured experimentally are averaged values, which precision depends on the measurement technique. Ideally, one should have a formalism that can integrate those macroscopic measurements, as well as the resolution scale of the recording. For all these reasons, it is justified to design mean-field models of LFPs (see details in Bedard and Destexhe, 2009,2011).

The first step to obtain a mean-field model of LFPs is to define macroscopic electric parameters, ϵ^M and σ^M, by taking an average of the "microscopic" electric parameters over some volume *Vol*, located at position $\vec{x}$:

$$\epsilon_\omega^M(\vec{x}) = < \epsilon_\omega(\vec{x}) >_{|Vol} = f(\vec{x}, \omega)$$

and

$$\sigma_\omega^M(\vec{x}) = < \sigma_\omega(\vec{x}) >_{|Vol} = g(\vec{x}, \omega) \ .$$

The typical order of magnitude of the volume *Vol* considered here will be around $10^3 \mu m^3$, which is much smaller than the typical volume of brain tissue. Consequently, these macroscopic electric parameters will depend on the position in the brain.

It is important to note that the macroscopic electric parameters σ^M and ϵ^M are frequency-dependent. This frequency dependence arises from the renormalization process, and is necessary for the macroscopic equations to be consistent [1]. It can be shown that different physical processes will result in different frequency dependence of these parameters. A perfectly resistive and homogeneous medium will result in no frequency dependence of σ^M and ϵ^M, while processes such as polarization, capacitive effects and ionic diffusion, will all lead to specific frequency-dependent profiles of σ^M and ϵ^M . For example, for a diffusive medium (a medium where ionic diffusion is taken into account), we have $\sigma^M + i\epsilon^M = k\sqrt{\omega}$ (where k is a complex number), for a polarizable medium we have $\sigma^M + i\epsilon^M = k(1 + i\omega\tau)$ (where k is a real number; see details in Bedard et al., 2006b; Bedard and Destexhe, 2009).

Defining similarly a macroscopic extracellular potential $< V_\omega >_{|Vol}$ by averaging V_ω over a volume Vol, leads to the following mean-field equation for V:

$$\nabla \cdot ((\sigma_\omega^M + i\omega\epsilon_\omega^M)\nabla < V_\omega >_{|Vol}) = 0 \, .$$

Solving this equation will give access to the macroscopic variations of V.

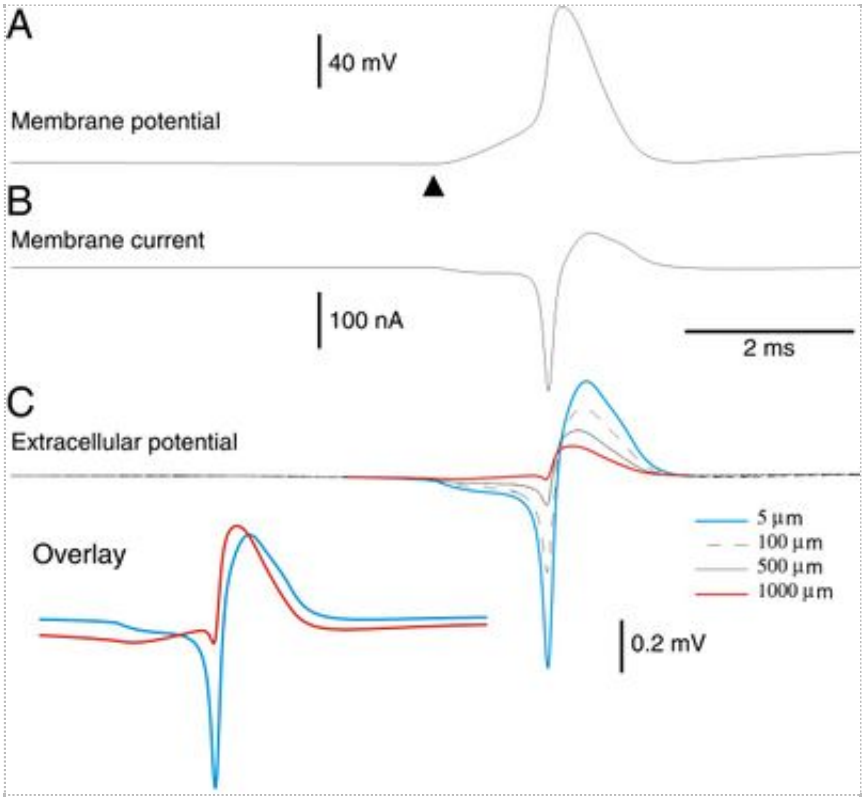

Figure 7: A model of the low-pass filtering properties of extracellular media. A. Membrane potential of a single-compartment model containing voltage-dependent Na^+ and K^+ conductances and a glutamatergic synaptic conductance. The glutamatergic synapse was stimulated at t = 5 ms (arrow) and evoked an action potential. B. Total membrane current generated by this model. Negative currents correspond to Na^+ and glutamatergic conductances (inward currents), while positive currents correspond to K^+ conductances (outward currents). C. Extracellular potential calculated at various distances from the source (5, 100, 500 and 1000 μm). The frequency filtering properties can be seen by comparing the negative and positive deflections of the extracellular potential. The fast negative deflection almost disappeared at 1000 μm (red) whereas the slow positive deflection was still present. The inset in C (Overlay) shows the traces at 5 (blue) and 1000 μm (red) overlayed (only the amplitude was scaled; modified from Bedard et al., 2004).

It is interesting to note that this equation has the same mathematical form compared to the microscopic model of the preceding sections. This form invariance is very useful, because one can introduce different physical phenomena (inhomogeneity, polarization, diffusion...) in the model, by simply introducing the corresponding frequency dependence of the macroscopic electric parameters σ_ω^M and ϵ_ω^M .

It is also important to keep in mind that the frequency dependences of the electrical parameters σ_ω^M and ϵ_ω^M cannot take arbitrary values, but are related to each-other by the Kramers-Kronig relations (Foster and Schwan, 1989; Kronig, 1926; Landau and Lifshitz, 1981). These relations are of course critical to relate the model to experiments, as shown previously (Jackson 1999; Gabriel et al., 1996).

Modeling the 1/f scaling of LFPs

As shown above, it was not possible to reconstruct the spectral properties of LFPs, and in particular the $1/f$ frequency scaling at low frequencies, from the unit activity using a resistive model (Fig. 5). A $1/f$ -filter was missing to explain the scaling properties of LFPs (Bedard et al., 2006a).

A plausible mechanism for this $1/f$ scaling was provided later based on the participation of ionic diffusion (Bedard and Destexhe, 2009, 2011). Using the macroscopic modeling approach outlined above, it was shown that ionic diffusion can give rise to a $1/f$ frequency scaling at low frequencies (Fig. 8). This is equivalent to postulate that there is a filter scaling as $1/\sqrt{\omega}$ (which will give $1/\omega$ in the power spectrum). This $1/\sqrt{\omega}$ is well-known in electrochemistry as the "diffusion impedance" or "Warburg impedance" (Diart et al., 1999; Taylor and Gileadi, 1995). Ionic diffusion appears, therefore, as a plausible physical mechanism to explain the $1/f$ spectral structure of LFPs, while being also consistent with the unit activity (Bedard and Destexhe, 2011) [2].

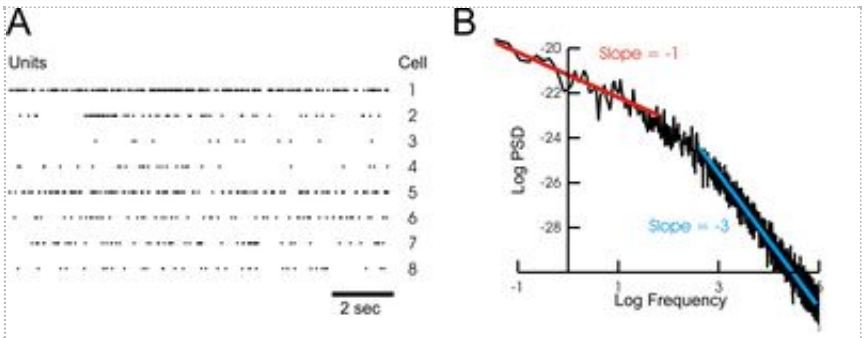

Figure 8: Successful reconstruction of LFP power spectra from unit activity when ionic diffusion is taken into account. A. Unit activity from awake cat (same as in Fig. 5C). B. PSD of the reconstructed LFP, taking into account ionic diffusion. The reconstructed LFP displays the same frequency scaling as the real LFP (compare with Fig. 5B; modified from Bedard and Destexhe, 2009).

Controversies about the sources of the LFP

To finish this review, it is interesting to mention a recent controversy concerning the possible contribution of electric monopoles in generating LFPs (Riera et al., 2012). Using a set of multi-contact electrodes inserted in the somatosensory cortex of the rat, these authors obtained recordings of neuronal activity in 3 dimensions, for both units and LFPs. In addition, these experiments included a detailed surface EEG recording of the rat brain. With these simultaneous recordings, the authors were able to establish first that the recordings do not obey instantaneously the electro-neutrality principle, suggesting the existence of monopolar sources. Such monopolar components might be an alternative explanation for previous results showing that dipole estimates realized from EEG or MEG (magnetoencephalogram) measurements do not match (Dehghani et al., 2010b).

In a second set of experiments, using a variant of the CSD analysis technique for data collected using linear probes (Nicholson and Freeman, 1975), Riera et al. (2012) quantified the relative contribution of the different multipolar components (monopoles, dipoles, quadrupoles, ...) to the scalp EEG data. Surprisingly, while there were significant dipolar and multipolar components as expected, they found an unexpected strong monopolar component. These data support prior evidence that in some cases, LFPs attenuate in $1/r$, as if they were generated by monopoles (Hunt et al., 2011). Riera et al. (2012) seem to confirm these preliminary observations.

In a commentary to this article (Destexhe and Bedard, 2012), several possible physical mechanisms were proposed to account for electric monopoles in neurons. It was pointed out that the neuronal membrane is very different from the electric circuit analogue of the membrane, which is widely used for modeling neurons. In particular, the mobility of charges (ions) is several order of magnitude lower than electrons, the charge carrier in an electronic circuit. The "ionic circuit", therefore, may not obey the well-known Kirchhoff's current laws, because charges will take a

significant time to start moving, and an inward current will not be instantaneously balanced by an outward current. Therefore, transient charge accumulation may occur, and will be seen transiently as electric monopoles. This interpretation has triggered some discussion, some authors arguing that monopoles are not consistent with the usual formalism for modeling neurons (Gratiy et al., 2013), while other authors pointed out that electric monopoles are possible but they require to use Maxwell equations without the usual approximations (Bedard and Destexhe, 2013).

The consequences of electric monopoles are potentially very important. Because monopolar sources predict a different attenuation ($1/r$) compared to dipoles ($1/r^2$), it will evidently impact our understanding of the genesis of LFP and EEG signals. If a given method to estimate neuronal activity from LFP or EEG assumes the wrong distance dependence, then this method will provide wrong estimates. It is tempting to relate this to the mismatch found by Dehghani et al. (2010b) for dipole estimates from EEG and MEG. If monopoles are present, the source estimates from EEG will be greatly affected and such estimation methods must be revised accordingly.

Future experimental work is necessary to confirm these observations of strong monopolar components in neurons. If confirmed, the presence of electric monopoles in neurons will have devastating consequences, not only to the interpretation of EEG/LFP or current source estimates, as explained above, but it will also require theoreticians to refine the current theories of electric phenomena in neurons. It may be that we have to profoundly revise our current models of neurons and population of neurons in a near future.

Conclusions

The LFP is a very important variable because it is available in many types of experimental recording configurations, ranging from glass micropipettes to multi-electrode arrays. Despite its widespread availability, the LFP is under-used because its biophysical origins remain incompletely understood. In this contribution, we have reviewed different properties of LFPs and different ways to model them. We reviewed simple models where the LFP is assumed to result from punctual (or line) current sources in a homogeneous resistive medium, as well as models taking into account more complex electrical properties of the extracellular medium.

The simple LFP model, where neurons are embedded in a uniform and resistive extracellular medium, is the one used in the vast majority of studies, and is therefore today's "standard model". This model provides an acceptable simulation of the LFP in many cases (e.g., Rall and Shepherd, 1968; Protopapas et al., 1998; Destexhe, 1998; Holt and Koch, 1999; Nunez and Srinivasan, 2005; Gold et al., 2006; Milstein et al., 2008; Pettersen and Einevoll, 2008; Linden et al., 2011). The procedures to implement this standard model are now available in popular simulators such as NEURON or GENESIS.

The fact of using resistive extracellular media is justified by some measurements (Logothetis et al., 2007), but it does not account for other measurements suggesting that the extracellular medium is non-ohmic (Gabriel et al., 1996; Bedard et al., 2010; Dehghani et al., 2010a; Wagner et al., 2013). But most importantly, the microstructure of extracellular space shows that it is far from being uniform, and rather consists of an aggregate of highly-conductive fluids with low-conductive membranes. There is therefore a serious possibility that the medium is more complex than a simple resistor, although this issue is still unclear today.

To account for such inhomogeneities, the standard model cannot be used, because the underlying formalism is only valid in resistive media. One must restart from first principles (Maxwell equations) to integrate electric parameters that depend on the spatial position in extracellular space. Such a formalism revealed that the inhomogeneities of

conductivity can give rise to strong filtering properties of LFPs (Bedard et al., 2004). Such a model should be used if one needs to account in detail for the attenuation of LFPs with distance. It was also shown that this model accounts for the characteristics of the current-source density (CSD) analysis of the slow oscillation in cerebral cortex (Bazhenov et al., 2011). Despite these important results, this model is too complex to apply in practice, because it requires to know in detail the 3D arrangement of fluids and membranes in the extracellular space around each neuron.

It must be noted that alternative mechanisms exist to explain the frequency filtering properties, in particular the very steep attenuation of the extracellular LFP signal of spikes. There can be a contribution of the low-pass filtering of the membrane (the "morphology filtering"; see Pettersen and Einevoll, 2008). This mechanism may explain a form of low-pass filtering, but seems incompatible with the $1/f$ scaling at low frequencies, and was also claimed to be negligible under ``in vivo--*like* conditions (Bedard et al., 2010). There can also be a contribution due to the fact that spikes may be quadrupoles (Milstein and Koch, 2008), and therefore have a steeper attenuation. Together with the filtering due to the extracellular medium, all these mechanisms contribute to filter the high frequency components of the LFP. The relative weight of these different mechanisms should be quantified by future experiments.

Another modeling formalism, easier to implement in practice, describes the tissue at a larger coarse-graining, and in which the electric parameters will be considered as an average over some volume of space, and thus are the result of a mixture of different media such as fluids and membranes. This mean-field model of LFPs (Bedard and Destexhe, 2009, 2011) also presents the advantage that it can directly incorporate macroscopic measurements of σ and ϵ in brain tissue (Gabriel et al., 1996). This approach also can integrate physical mechanisms such as ionic diffusion, which turns out to be the one that explains various measurements including the $1/f$ scaling properties of LFPs at low frequencies (Fig. 8). This mean-field approach can also be applied to generalize the CSD analysis (which is only valid in resistive media) to extracellular media with arbitrarily complex electrical properties (Bedard and Destexhe, 2011). Such models can also integrate electric monopoles, and thus, we expect that mean-field LFP models will play an increasingly important role in the future.

Footnotes

1. Intuitively, we can see that if a given medium is a low-pass filter because of inhomogeneities of σ and ϵ, then if we take the system at a more macroscopic level, it has to remain a low-pass filter. The only way to keep this property is that σ^M and ϵ^M are frequency dependent.
2. There is presently no other theory that can explain all the data in a coherent framework.

References

- Bazhenov M, Lonjers P, Skorheim P, Bedard C and Destexhe A. (2011) Non-homogeneous extracellular resistivity affects the current-source density profiles of up-down state oscillations. Phil Trans R Soc A 369: 3802-3819.
- Bhattacharya, J., and H. Petsche. (2001) Universality in the brain while listening to music. Proceedings:

Biological Sciences 268: 2423-2433.

- Bedard, C., Kroger, H. and Destexhe, A. (2004) Modeling extracellular field potentials and the frequency-filtering properties of extracellular space. Biophys. J. 86: 1829-1842.
- Bedard, C., Kroger, H. and Destexhe, A. (2006a) Does the 1/f frequency scaling of brain signals reflect self-organized critical states ?. Physical Review Lett. 97: 118102.
- Bedard, C., Kroger, H. and Destexhe, A. (2006b) Model of Low-Pass Filtering of Local Field Potentials in Brain Tissue Physical Review E 73 :051911.
- Bedard, C. and Destexhe, A. (2009) Macroscopic models of local field potentials and the apparent 1/f noise in brain activity. Biophys. J. 96: 2589-2603.
- Bedard, C. and Destexhe, A. (2011) A generalized theory for current-source density analysis in brain tissue. Physical Review E 84: 041909.
- Bedard, C. and Destexhe, A. (2013) Electric monopoles are indeed compatible with Maxwell equations. J. Neurophysiol. 109: 1683.
- Bedard, C., Rodrigues, S., Roy, N., Contreras, D. and Destexhe, A. 2010. Evidence for frequency-dependent extracellular impedance from the transfer function between extracellular and intracellular potentials. J. Computational Neurosci. 29: 389-403.
- Beggs, J., and Plenz, D. (2003) Neuronal avalanches in neocortical circuits. J. Neurosci.. 23 : 11167-11177.
- Berger H. (1929) Uber den zeitlichen verlauf der negativen schwankung des nervenstroms. Arch. Ges. Physiol. 1: 173.
- Bishop, G.H. (1936) The interpretation of cortical potentials. Cold Sping Harbor Symp. Quant. Biol. 4: 305-319.
- Bremer, F. (1938) L'activité électrique de l'écorce cérébrale. Actualités Scientifiques et Industrielles 658: 3-46.
- Bremer, F. (1949) Considérations sur l'origine et la nature des "ondes" cérébrales. Electroencephalogr. Clin. Neurophysiol. 1: 177-193.
- Creutzfeldt, O., Watanabe, S. and Lux, H.D. (1966a) Relation between EEG phenomena and potentials of single cortical cells. I. Evoked responses after thalamic and epicortical stimulation. Electroencephalogr. Clin. Neurophysiol. 20: 1-18.
- Creutzfeldt, O., Watanabe, S. and Lux, H.D. (1966b) Relation between EEG phenomena and potentials of single cortical cells. II. Spontaneous and convulsoid activity. Electroencephalogr. Clin. Neurophysiol. 20: 19-37.
- Dehghani, N, Bedard, C., Cash, S.S., Halgren, E. and Destexhe, A. (2010a) Comparative power spectral analysis of simultaneous elecroencephalographic and magnetoencephalographic recordings in humans suggests non-resistive extracellular media. J. Computational Neurosci. 29: 405-421.
- Dehghani N, Cash SS, Chen CC, Hagler DJ Jr, Huang M, Dale AM and Halgren E. (2010b) Divergent cortical generators of MEG and EEG during human sleep spindles suggested by distributed source modeling. PLoS One 5: e11454.
- Dehghani, N., Hatsopoulos, N.G., Haga, Z.D., Parker, R.A., Greger, B., Halgren, E., Cash, S.S. and Destexhe, A. (2012) Avalanche analysis from multi-electrode ensemble recordings in cat, monkey and human cerebral cortex during wakefulness and sleep. Frontiers Physiol. 3: 302.
- Destexhe, A. (1998) Spike-and-wave oscillations based on the properties of $GABA_B$ receptors. J. Neurosci. 18: 9099-9111.

- Destexhe, A. and Bedard, C. (2012) Do neurons generate monopolar current sources ? J. Neurophysiol. 108: 953-955.
- Destexhe, A., Contreras, D. and Steriade, M. (1999) Spatiotemporal analysis of local field potentials and unit discharges in cat cerebral cortex during natural wake and sleep states. J. Neurosci. 19: 4595-4608.
- Diard, J-P., Le Gorrec, B. and Montella, C. (1999) Linear diffusion impedance. General expression and applications. J. Electroanalytical Chem. 471: 126-131.
- Eccles, JC. (1951) Interpretation of action potentials evoked in the cerebral cortex. J. Neurophysiol. 3: 449-464.
- Foster, K.R. and Schwan, H.P. (1989) Dielectric properties of tissues and biological materials: a critical review. Crit. Reviews Biomed. Engineering. 17: 25-104.
- Gabriel, S., Lau, R.W. and Gabriel, C. (1996) The dielectric properties of biological tissues : II. Measurements in the frequency range 10 Hz to 20 GHz. Phys. Med. Biol.. 41: 2251-2269.
- Gold, C., Henze, D.A, Koch, C. and Buzsaki, G. (2006) On the origin of the extracellular action potential waveform: A modeling study. J. Neurophysiol.. 95: 3113-3128.
- Gratiy, S.L., Pettersen, K.H., Einevoll, G.T. and Dale, A.M. (2013) Pitfalls in the interpretation of multielectrode data: on the infeasibility of the neuronal current-source monopoles. J. Neurophysiol. 109: 1681-1682.
- Holt,G.R. and Koch, C. (1999) Electrical interactions via the extracellular potential near cell bodies. J Comput. Neurosci. 6: 169-184.
- Hunt MJ, Falinska M, Leski S, Wojcik DK and Kasicki S. (2011) Differential effects produced by ketamine on oscillatory activity recorded in the rat hippocampus, dorsal striatum and nucleus accumbens. J. Psychopharmacol. 25: 808-821.
- Jackson, J.D. (1999) Classical Electrodynamics, Third edition. John Wiley and Sons, New York.
- Jensen, H.J. (1998) Self-Organized Criticality. Emergent Complex Behavior in Physical and Biological Systems. Cambridge University Press, Cambridge, UK.
- Katzner, S., Nauhaus, I., Benucci, A., Bonin, V., Ringach, D.L. and Carandini M. (2009) Local origin of field potentials in visual cortex. Neuron. 61: 35-41.
- Klee, M.R., Offenloch, K. and Tigges, J. (1965) Cross-correlation analysis of electroencephalographic potentials and slow membrane transients. Science 147: 519-521.
- Kronig, R.D.L.. (1926) On the theory of dispersion of X-rays. J. Opt. Soc. Am.. 12: 547.
- Landau, L.D. and Lifshitz, E.M. (1981) *Electrodynamics of Continuous Media*. Pergamon Press, Moscow, Russia.
- Linden, H., Pettersen, K.H. and Einevoll, G.T. (2010) Intrinsic dendritic filtering gives low-pass power spectra of local field potentials. J. Comput. Neurosci. 29: 423-444.
- Linden, H., Tetzlaff, T., Potjans, T.C., Pettersen, K.H. Grun, S., Diesmann, M. and Einevoll, G.T. (2011) Modeling the spatial reach of the LFP. Neuron 72: 859-872.
- Logothetis, NK, Kayser, C. and Oeltermann, A. (2007) In vivo measurement of cortical impedance spectrum in monkeys: Implications for signal propagation. Neuron 55: 809-823.
- Milstein JN and Koch C. (2008) Dynamic moment analysis of the extracellular electric field of a biologically realistic spiking neuron. Neural Comput. 20: 2070-2084.
- Novikov, E., Novikov, A. Shannahoff-Khalsa, D., Schwartz, B. Wright, J. (1997) Scale-similar activity in the brain. Phys. Rev. E. 56: R2387-R2389.

- Niedermeyer, E. and Lopes da Silva, F. (editors) (1998) *Electroencephalography* (4th edition), Williams and Wilkins, Baltimore.
- Nunez, P.L. and Srinivasan, R. (2005) *Electric Fields of the Brain*. (2nd ed) Oxford university press, Oxford, UK.
- Peters, A., Palay, S.L. and Webster, H.F. (1991) *The fine Structure of the Nervous System*. Oxford University Press, Oxford, UK.
- Pettersen, K.H. and Einevoll, G.T. (2008) Amplitude variability and extracellular low-pass filtering of neuronal spikes. Biophys J. 94: 784-802.
- Peyrache, A., Dehghani, N., Eskandar, E.N., Madsen, J.R., Anderson, W.S., Donoghue, J.S., Hochberg, L.R., Halgren, E., Cash, S.S., and Destexhe, A. (2012) Spatiotemporal dynamics of neocortical excitation and inhibition during human sleep. Proc. Natl. Acad. Sci. USA 109: 1731-1736.
- Pritchard, W.S. (1992) The brain in fractal time: 1/f-like power spectrum scaling of the human electroencephalogram. Int. J. Neurosci. 66, 119-129.
- Protopapas, A.D., Vanier, M. and Bower, J. (1998) Simulating large-scale networks of neurons. In: *Methods in Neuronal Modeling* (2nd ed), C. Koch and I. Segev, editors. MIT Press, Cambridge MA. 461-498.
- Rall, W. and Shepherd, G.M. (1968) Theoretical reconstruction of field potentials and dendrodendritic synaptic interactions in olfactory bulb. J. Neurophysiol. 31: 884-915.
- Riera, J.J., Ogawa, T., Goto, T., Sumiyoshi, A., Nonaka, H., Evans, A., Miyakawa, H. and Kawashima, R. (2012) Pitfalls in the dipolar model for the neocortical EEG sources. J. Neurophysiol 108: 956-975.
- Rothberger F (1931) cited in: Bremer, F. (1938) L'activité électrique de l'écorce cérébrale. Actualités Scientifiques et Industrielles 658: 3-46.
- Steriade M. (2003) *Neuronal Substrates of Sleep and Epilepsy*. Cambridge University Press, Cambridge, UK.
- Steriade M, Timofeev I and Grenier F. (2001) Natural waking and sleep states: a view from inside neocortical neurons. J. Neurophysiol. 85: 1969-1985.
- Taylor, S.R. and Gileadi, E. (1995) The physical interpretation of the Warburg impedance. Corrosion 51: 664-671.
- Wagner, T., Eden, U., Rushmore, J., Russo, C.J., Dipietro, L., Fregni, F., Simon, S., Rotman, S., Pitskel, N.B., Ramos-Estebanez, C., Pascual-Leone, A., Grodzinsky, A.J., Zahn, M. and Valero-Cabre, A. 2013. Impact of brain tissue filtering on neurostimulation fields: A modeling study. NeuroImage, in press.

Further Reading

- Brette R. and A. Destexhe, editors. (2012) *Handbook of Neural Activity Measurement*, Cambridge University Press, Cambridge, UK.
- Koch, C. and I. Segev, editors. (1998) *Methods in Neuronal Modeling* (2nd ed). MIT Press, Cambridge MA.

Internal links

Electroencephalogram

Fast oscillations

General anaesthesia

High-conductance state

Neural fields

Spike-and-Wave oscillations

Thalamocortical oscillations

Up and Down states

Volume conduction

Sponsored by: Eugene M. Izhikevich, Editor-in-Chief of Scholarpedia, the peer-reviewed open-access encyclopedia
Reviewed by (http://www.scholarpedia.org/w/index.php?title=Local_field_potential&oldid=135758) : Dr. Axel Hutt, INRIA, Villers-les-Nancy, France
Reviewed by (http://www.scholarpedia.org/w/index.php?title=Local_field_potential&oldid=0) : Eugene M. Izhikevich, Editor-in-Chief of Scholarpedia, the peer-reviewed open-access encyclopedia
Accepted on: 2013-08-26 18:53:11 GMT (http://www.scholarpedia.org/w/index.php?title=Local_field_potential&oldid=135811)